Lappeenranta University of Technology
School of Computational Engineering
Degree Program in Technical Physics

Nafiseh Mohammadi

HUMIDITY TO ELECTRICITY CONVERTER BASED ON ZIRCONIA NANO-PARTICLES

Examiners: Professor Erkki Lähderanta
Researcher Pavel Geydt

Supervisors: Professor Erkki Lähderanta
Researcher Pavel Geydt

ABSTRACT

Lappeenranta University of Technology
School of Computational Engineering
Degree Program in Technical Physics

Nafiseh Mohammadi

HUMIDITY TO ELECTRICITY CONVERTER BASED ON ZIRCONIA NANO-PARTICLES

Master's Thesis

40 pages, 24 figures, 5 tables

Examiners: Professor Erkki Lähderanta
Researcher Pavel Geydt

Keywords: Zirconia Oxide, Monoclinic, Tetragonal, Cubic, water adsorption, YSZ, hygroelectricity, nanocomposites, AFM, SEM, TZP, Vapour deposition, lithography, heat-treated.

Conversion of electrochemical energy to the electric energy through interaction of the ZrO2-based nanocomposite with atmospheric humidity for different composition was investigated. Also, involved factors on producing energy in this method by measuring output voltage for open circuit and circuit with load of 1MΩ under different humidity and temperature condition and for different weight portion of nanoparticles was studied. SEM imaging and EDS spectroscopy of the nanocomposite indicates that amount of output voltage has a direct relation with agglomeration of nanoparticles on the nanocomposite.

ACKNOWLEDGEMENTS

Special thanks to my supervising professor Erkki Lähderanta who gives me the opportunity to be a part of this study and support me throughout the studding in LUT. I would like to also express my gratitude to Dr. Andrey Lyubchik who willingly teach and guide me during this study.

Finally, I acknowledge funding by the HUNTER project (grant nº 691010).

Lappeenranta, August 2017

Nafiseh Mohammadi

Table of Contents

LIST OF SYMBOLS AND ABBREVIATIONS

AFM	Atomic Force Microscopy
DFM	Dimethylformamide
EDS	Energy Dispersive Spectroscopy
KPFM	Kelvin Probe Force Microscopy
PMMA	Poly (methyl methacrylate)
TEM	Transmission Electron Microscopy
TZP	Tetragonal Zirconia Polycrystalline
UV	Ultraviolet
YSZ	Yttria Stablized Zirconia

1 INTRODUCTION

Growth of global population and industry as well as increase of using different machines in our daily life caused a continuous growing in demand for energy. On the other hand, global warming, ecological issues and decreasing fossil fuel resources, put restriction on our tradition way of producing energy. Accordingly, all over the world broad study on different sources of energy such as geothermal, solar, wind, and biofuel is trying to find alternative sources. Among them, hygroelectricity [1] is one of the most recent candidates to obtain clean energy. In this method humidity was assumed to be converted into electrical energy. This phenomenon can be utilized to produce power by scavenging electrical energy from the atmosphere.

1.1. Background

The first impression is that in high humidity electro statistic charge tends to disappear. But interestingly, in 2008 for the first time it was observed that positive potential of the charged acrylic sheet can cause accumulation of negative ions on cellulose film and produces zero potential under controlled relative humidity [1]. This phenomenon can be explained by neither the usual induction model nor by water molecular dipole orientation, as it appears much faster with very short relaxation time of the order of microsecond. On the other hand, due to electrochemical potential ($\mu_i = \mu_i^0 + RTln\, a_i + z_{FV}$), atmospheric water adsorbed on the insulator produces excess of ions, $H^+(H_2O)_n$ and $OH^-(H_2O)_n$ which is trapped within the solid surface and bulk.

In other research in 2010, Ducati [2] showed that the exposure of isolated metal samples to water vapor leads to the deposition of excess of negative or positive charge on the metal. Creation of charges is highly dependent on relative humidity and is caused by OH^- and H^+ ions transfer to gas-solid interfaces. In the following works [3&4] a research group of MIT in 2014 observed that merged water droplets on the surface of super-hydrophobic nanostructured surfaces can spontaneously jump from the surface due to the release of excess surface energy. They did an experiment on nanostructured super-hydrophobic CuO and hydrophilic Cu combs. It was observed that these jumping droplets were positively charged (10–100 fC) [5], which then can be manipulated with electric field. The creation of charge

is caused by Electric-double-layer charge separation at the hydrophobic coating interface [5].

The recent study [6] developed and investigate more deeply an innovative humidity-to-electricity conversion system, in which the designed testing device works based on compressed tetragonal YSZ (TZP), ZrO2+3mol%Y2O3 (9 nm). In this system TZP Nano powder was compressed in form of tablet with 20 mm diameter and height of 2-3 mm, **Fig.1**,

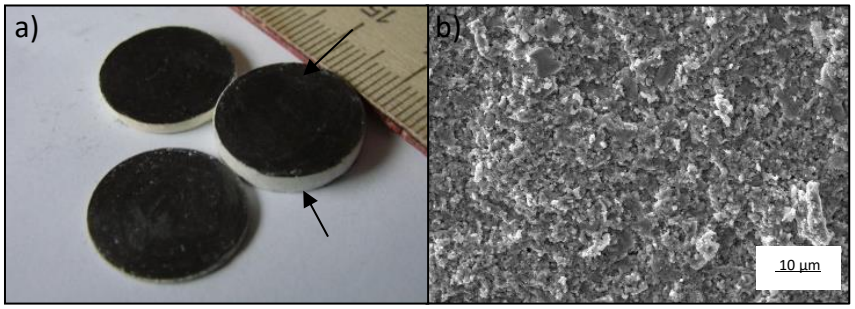

Fig 1. Photo and TEM images of TZP Nano powder tablets [6].

with graphite electrodes deposited mechanically on the sides of the tablets. The saturated tablets by humidity then place in a circuit with a load of 1MΩ, after 20 min the potential difference (measured by digital voltmeter) between the electrodes V(t) increases up to 60 mV.

1.2. Structure of the thesis

This thesis includes 5 main sections, in the first section there is a short background and history related to the current study. Seconded section includes three subsections, first one includes description of zirconia and its properties in different phases and also water adsorption is discussed in this part. The second subsection is related to practical part of the study and comprised of different subsections describing topics from preparation of the samples and experimental setups. In third subsection different measurement, result and analysis get discussed. Discussion and conclusion and summery are mentioned as third and fourth main sections and fifth section is named references.

2 THESIS

2.1 MATERIAL AND THEIR PROPERTIES

In this section a short description on structure and properties of different materials which are related or used during the study is mentioned. Zirconia oxide in its three different phases and yttria-stabilized zirconia and also mechanism of water adsorption in them are shortly described.

2.1.1 ZIRCONIUM OXIDE

Zirconium dioxide, ZrO_2, known as zirconia with density of 5.68 g cm^{-3}, melting point of 2715 °C, and boiling point of 4300 °C draw much attention due to its unique properties. It possesses weak acid and basic sites and shows stability under oxidizing. It can be found in three different phases: monoclinic, tetragonal and cubic. With temperature arising, two phase transitions can be observed (**Fig. 2**), around 1205°C, its phase change from monolithic to

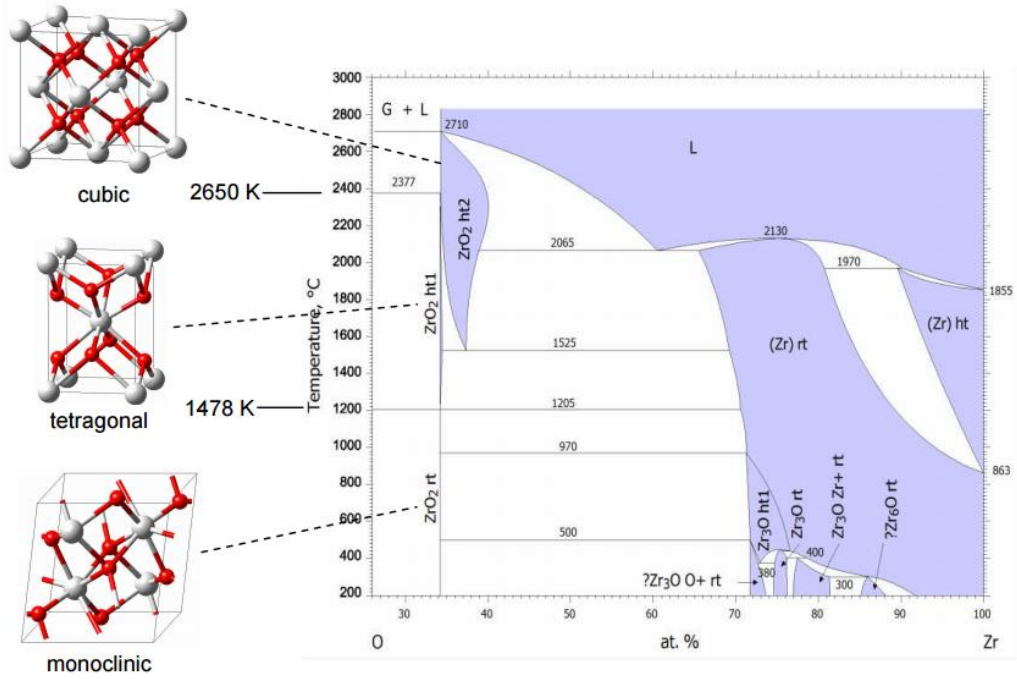

Fig 2. Phase diagram of O-Zr. ZrO2 is in monoclinic phase in the room temperature (rt), at the high temperature (ht1) above 1478 K or 1205°C tetragonal phase and a transition to cubic phase is observed at the high temperature 2650 K or 2377°C (ht2). [7]

tetragonal and at about 2377°C its molecular structure change to cubic. Due to having large volume change in transition from monoclinic to tetragonal phase, some cracks might appear in a sample made of pure zirconia and it might be shattered. To avoid this phenomenon, tetragonal and cubic zirconia can be stabilized at room temperature either by doping with aliovalent oxides such as yttria (Y_2O_3), calcia (CaO) and magnesia (MgO) [8], or by particle size reduction [5].

In its monoclinic phase each unit of zirconia consist of 4 zirconium atoms and 8 oxygen atoms, whose combination represents a face centered structure. There is nine different crystalline directions: [001], [010], [100], [110], [101], [011], [1 ¯01], [111] and [1 ¯11].

The molecular structure of cubic zirconia is calcium fluorite (CF_2) with lattice parameter of 0.517 nm. Zirconium atoms are located at the corners and halves of <110> direction of a cubic cell, while oxygen atoms are placed at quarts of <111 > direction. In cubic phase zirconia has high ionic conductivity comparing to other phases because it has equal oxygen vacancy sites in all directions of the lattice structure [9].

By the movement of oxygen anions (O^{2-}) along one of the cubic axes the tetragonal zirconia

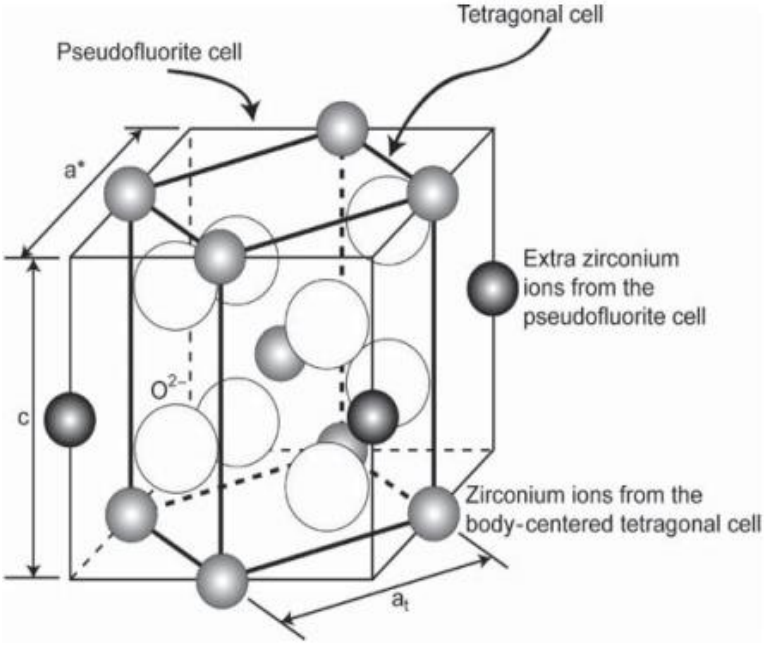

Figure 3. Tetragonal zirconia unit cell [10].

is derived from the cubic fluorite structure **Fig.3** [10]. In the transition from cubic to tetragonal phase four Zr^{4+} cations which place at the 4a cubic positions split and move to the 2b positions, also the O^{2-} anions in the 8c cubic positions divide into two groups and then

occupy the 4d positions in the tetragonal structure. Axes a and b directed in 45° from those in cubic cell in the tetragonal lattice and axis c is the same in both structures.

2.1.2 YTTRIA-STABILIZED ZIRCONIA (YSZ)

Zirconia phase can be stabilized by different dopant, the most commonly used dopant to stabilize the cubic and tetragonal phase of zirconia is yttria. Yttria-stabilized zirconia (YSZ) is an oxide material, which has found wide range of application from thermal barrier coating to electrolyte in solid fuel cells and in catalysis. It shows high mechanical strength, resist to radiation and corrosion, chemically is stable and it is a fast-ion conductor in high temperature due to oxygen vacancies. Stabilizing improves different properties such as strength, toughness and thermal-shock resistance. From **Fig.4** it can be observed that with

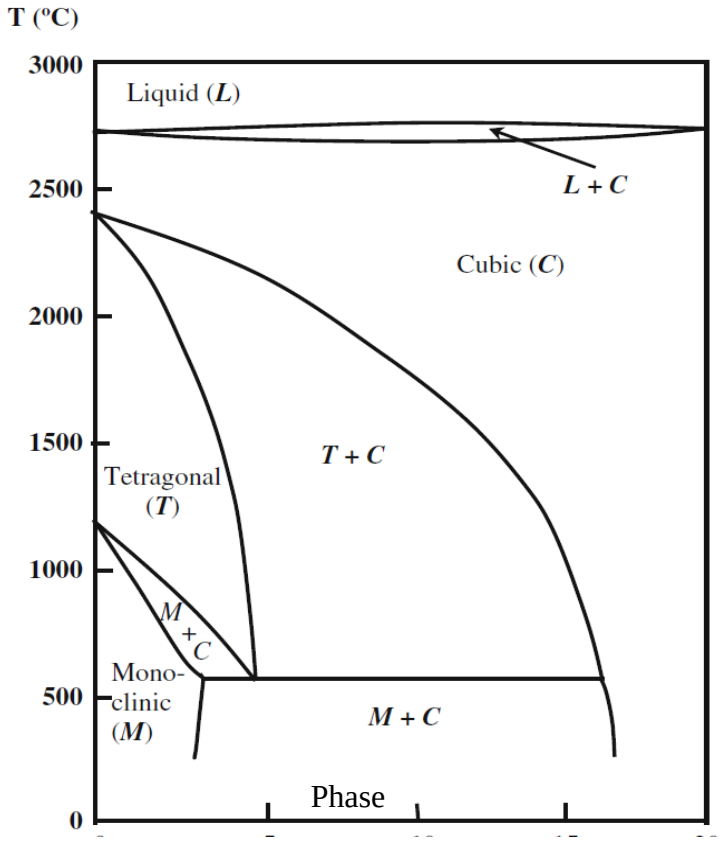

Figure 4. Tetragonal and fully cubic (F) phase of zirconia can be stabilized down to room temperature with yttria as dopant. Tetragonal phase is stabilized with dopant concentration between 2 mole% and 6.5 mole% and fully cubic (F) with concentration more than 6.5 mole% [10].

concentration more than 7 mole% a fully cubic stabilized zirconia can be obtained and with concentration between 2 mole% to about 7 mole% tetragonal phase can be stabilized (TZP) down to room temperature [11].

Main responsible factor for stabilizing zirconia is taught to be anion vacancies. Due to having lower valence than zirconium ion (Zr^{4+}), Y^{3+} cation induces oxygen vacancies to compensate charge. For instance, by substitution of Zr^{4+} with Y^{3+} a net negative charge in the lattice is created in a way that an oxygen vacancy is formed for every mole of yttria incorporated into the zirconia lattice. In order to keep charge neutrality, either anion vacancies or cation interstitials must be formed. The cations of oxides stabilize the cubic form or tetragonal phase of zirconia down to room temperature.

Zirconia stabilized with approximately 3% yttria is called tetragonal zirconia polycrystalline (TZP). In this form at room temperature the polycrystalline is almost 100% tetragonal, so its grade possess the highest toughness at room temperature.

2.1.3 WATER ADSORBTION ON TETRAGONAL ZIRCONIA

When zirconia is in its tetragonal phase and exposed to an external effects, its tetragonal phase may transform to monoclinic one. This transformation is an exothermic interaction and changes the physical and mechanical properties of the material. For the first time in 1981 it was shown that that in presence of moisture, yttria-stabilized zirconia ceramics would slowly change from the tetragonal to monoclinic phase at room temperature which then decelerates with increase in temperature. This phenomenon is known as low-temperature degradation (LTD) due to reduction in strength of the ceramic. [Diffusion of Water Species in Yttria-Stabilized Zirconia].

When physically or chemically water molecules are adsorbing on tetragonal zirconia, surface of the powder or ceramic will act as sorbents. This adsorption can effect on wave functions of the lattice and disturbing the lattice potential periodicity which then might causes discrete donor or acceptor levels to place in the tetragonal-ZrO2 forbidden gap. This cause that that yttrium acceptor move above the Fermi level and strength of the vacancy–yttrium ionic bond changed. Accordingly, the distance between atoms of zirconium and yttrium will change and the material experiences phase shift form tetragonal to monoclinic, the enthalpies of this transition is 5.272±0.544 kJ/mol [12-13].

2.2 SAMPLE PREPARATION

Procedure of preparation of the samples includes applying thin film of aluminum on glass substrate through vacuum evaporation deposition, printing of pattern with positive lithography method and applying a solution containing nanoparticles on the surface of electrodes by aerosol spraying method.

2.2.1 ALUMINUM DEPOSITION

Thin film of aluminum was deposited on a glass substrate through Vacuum Evaporation method. In this method material, which is going to be deposited evaporates and then condenses on surface of the substrate. In detail, the procedure includes cleaning substrate glasses in sonic bath with acetone and isopropanol, each for 15 minutes respectively, then samples get dried with pressurized nitrogen. Four completely clean glasses each in size of 10*10 (cm2) (**Fig.5** A, B) installed inside the chamber, (Fig.5 C) above "boat", containing a small piece of aluminum, boat is a small container to keep martial which is going to be deposited on top of the glass. Then the system gets locked and vacuumed to reach to pressure of 10^{-4} bar which will be followed to deep vacuum. Having the pressure around 10^{-9} bar, with passing high current or voltage, the piece of aluminum start to be melted, evaporated and condensed on top of the glasses. During the process of evaporation and then deposition, a sensor indicating rate of deposition must be watched out. Finally, when rate of deposition dropped, current or voltage needs to be switched off and pressure gradually increased to atmospheric pressure. In this method position of substrate as well as quality of the vacuum and purity of the source material affect thickness of deposited film. Thickness of deposited aluminum is measured in different places as it is marked in **Fig.5**A, with profilometer and it differs from 30 nm to 150 nm considering the position of the glasses in regard to the front door. Thickness follows the decreasing trend from sample number 3 to 1 and 4 to 2, top to the bottom of **Fig.5**A, also 3 to 4 and 1 to 2, left to right of **Fig.5**A.

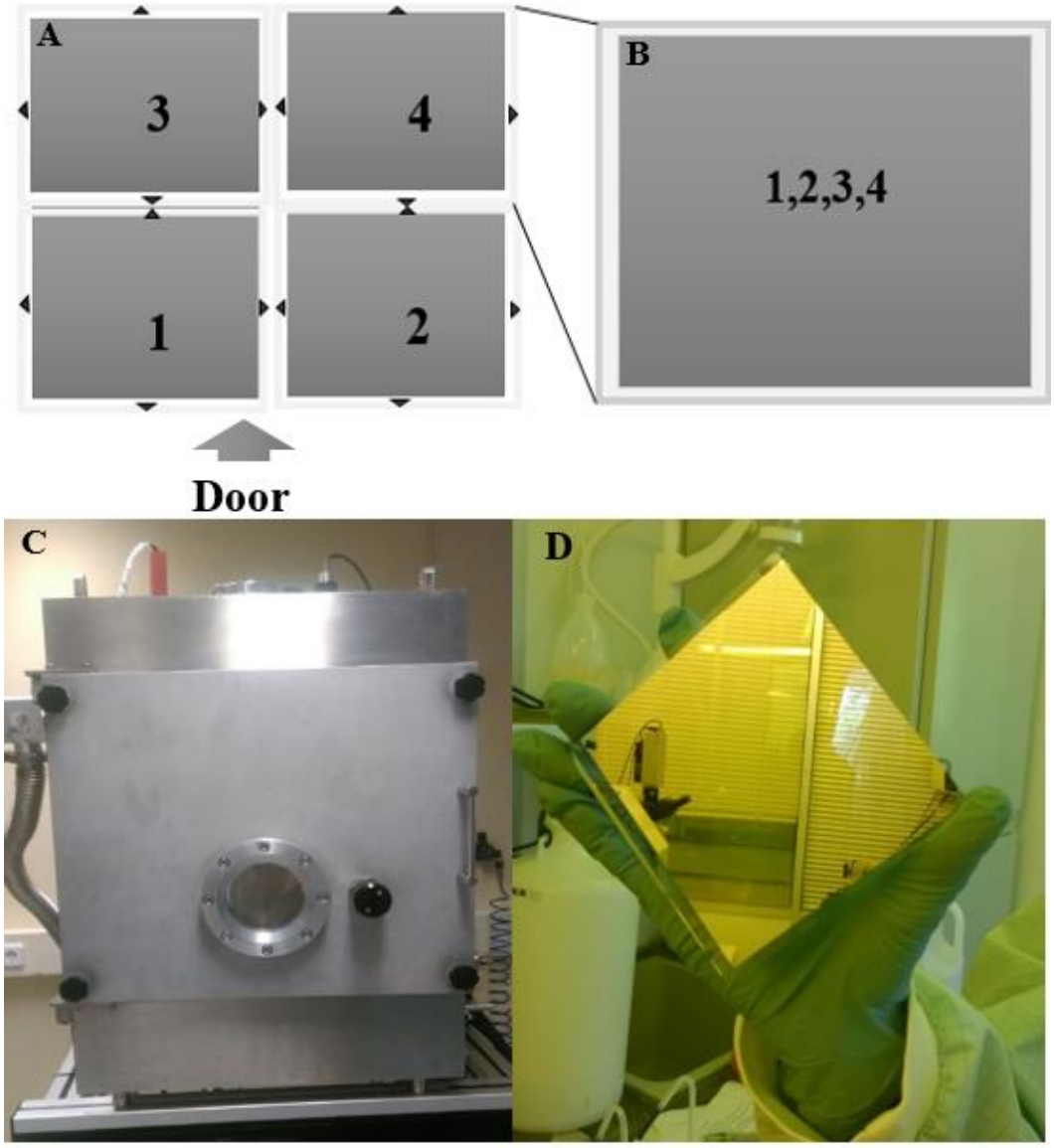

Fig.5. A: Four clean glass get fixed to be placed in the chamber. The thickness of marked position got measured. B: Each glass sized 10*10 (cm). C: Chamber for deposition. D: A glass after deposition of aluminum.

2.2.2 LITHOGRAPHY

To transfer pattern of electrodes on the aluminum plates, lithography was used. In this method surface of the plates needs to be covered by photoresist liquid. Photoresists are light sensitive material which considering their reaction with UV light are divided into two main category, positive and negative. As it can be seen from **Fig.6**, in the case of positive photoresists, exposure to UV light changes chemical structure of the liquid and makes it more soluble while when negative photoresist exposed to UV polymerized and become extremely difficult to dissolve [14].

In our experiment, using spin coating machine a thin layer of AZ6632 photoresist liquid, positive photoresist, was applied on top of the clean aluminum substrate, type of photoresist is selected considering the thickness of the layer they need to be protected against UV light [15]. Speed of the spinner needs to be defined and controlled according to the kind of photoresist. After spinning the sample get baked for one minute on 115ºC hot plate and left to cool down. Pre-designed mask was placed on top of the sample and then it was exposed to UV light in mask-liner machine for a minute. After this stage a parts of deposited photoresist which was placed in transparent part of the mask, gets removed through developing with KOH and water. This stage get followed by etching aluminum from the parts without photoresist. Suitable etchant for aluminum is $H_3PO_4^+$ HNO_3^+ H_2O at 40 °C without agitation and it needs to be stopped when all uncovered aluminum is removed from surface. Finally it is rinsed with water and isopropanol and a well printed pattern on the glass substrates obtained which then needed to be cut with laser according its pattern.

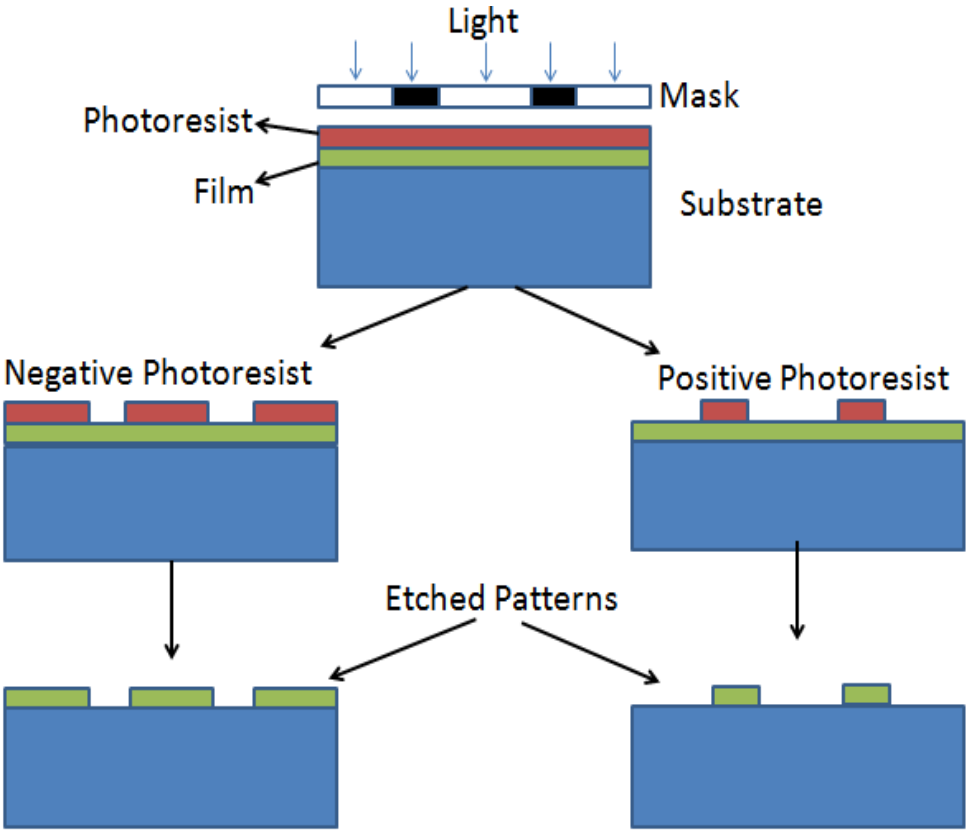

Fig 6. Procedure of lithography in both cases of positive and negative lithography [14].

2.2.3 SCANNING ELECTRON MICROSCOPY (SEM)

The Scanning Electron Microscopy (SEM) comprise of electron gun (source), magnetic electron lenses, sample stage, different detectors for variable signals etc. SEM utilizes at least one detector, which is mostly used to detect secondary electrons Fig.7.A.

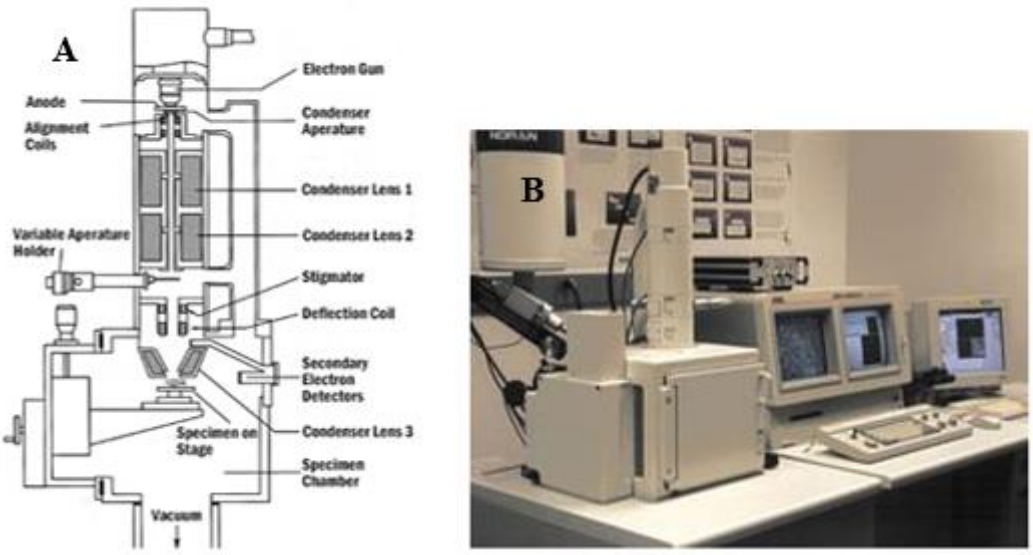

Fig.7.A**:** Schematic view of SEM instrument, B: Photo of SEM instrument [17].

SEM produces and focuses high energy beam of electrons by a series of electromagnetic lenses in the SEM column to produce signals on the surface of solid specimens. The signal is generated due to electron-sample interactions and they include secondary electrons (that produce SEM images), backscattered electrons (BSE), diffracted backscattered electrons (EBSD), characteristic X-rays, visible light and heat.

Backscattered electrons are referred to elastic collision of an incident electrons, which typically occurs due to collision of incident electron with a sample atom's nucleus. They possess energy of same level as the incident electrons. On the other hand, inelastic scattered electrons have lower energy, about 50 eV or less, and are called secondary electrons. They can either formed by the emission of loosely bound electrons of sample atoms or by collisions with the nucleus where energy loss occurs. Morphology and topography of the samples is detected by secondary electrons and backscattered electrons are utilized to show contrasts in composition in multiphase samples.

In addition, inelastic collisions of the incident electrons with electrons in discrete orbitals of atoms might excite an electron, then with returning it to lower energy level X-ray with fixed wavelength (which is related to the difference in energy levels of electrons in different shells for a given element) can be generated, which then can be used to find out chemical element as component of the sample [17, 18].

2.2.4 PREPRATION OF THE SOLUTION

Solution that was planned to be applied on the surface of samples composed of poly methylmethacrylate (PMMA), diluted with dimethylformamide (DMF), in portion of 1 to 10 of their weight and different weights of $Z_2O_2 - 3Y_2O_3$ nanoparticles . In several flasks, each 0.250 g of Polycarbonate (PC) got added to 5 ml of the above mentioned solution. According to the predefined plan of the experiment, different weight of $Z_2O_2 - 3Y_2O_3$ nanoparticles get mixed with the solution in order to have different concentration of nanoparticles considering the weight of PMMA, the percentage ranged from 10 to 150%.

2.2.4.1 POLY METHYLMETHACRYLATE (PMMA)

PMMA was developed for the first time in 1928 from polymerization of methyl methacrylate [19]. PMMA with chemical formula of $C_5H_8O_2$, is a transparent thermoplastic and is known as acrylic glass. Due to its lightweight and shatter-resistance, it is used in sheet form as an alternative to glass. In the presented study this material is selected to be one of the compound as it is a suitable candidate to act as pore-forming agent in YSZ ceramic [20].

2.2.4.2 DIMETHYLFORMAMIDE

DMF is an organic, colorless, liquid with chemical formula of $(CH_3)_2NC(O)H$. It is known as a universal solvent and is widely used as a solvent, catalyst and reagent in the synthetic organic chemistry. Because of possessing high dielectric constant, and low volatility, it has wide applicability in chemical reactions, which require a high solvency power [19].

2.2.5 DEPOSITION OF THE SOLUTION ON THE SAMPLES

The utilized method for deposition of the solution on top of the electrodes was aerosol spraying. In this method, an airbrush connected to pressurized nitrogen and a bottle of solution is installed on top of the heater (**Fig.8**A & C). The procedure includes frequent spraying with a rest time to let the deposited layer get dried on top of the substrate (**Fig. 8**E).

Considering the result from previous study, the pressure of the nitrogen needs to be adjusted in 2 bar and heater needed to reach temperature of 120℃ , the optimum distance between the air brush and the substrate (to reach a uniform deposition over $2cm^2$) obtained to be ~45 cm and each spray lasted for a second with rest time of 1 minute for the first time and 30 second for further iterations. Two samples were fabricated for each concentration of nanoparticles: one was supposed not to have nanoparticles on its edges electrodes and contacts and the other was covered with the solution in all parts except metallic contacts

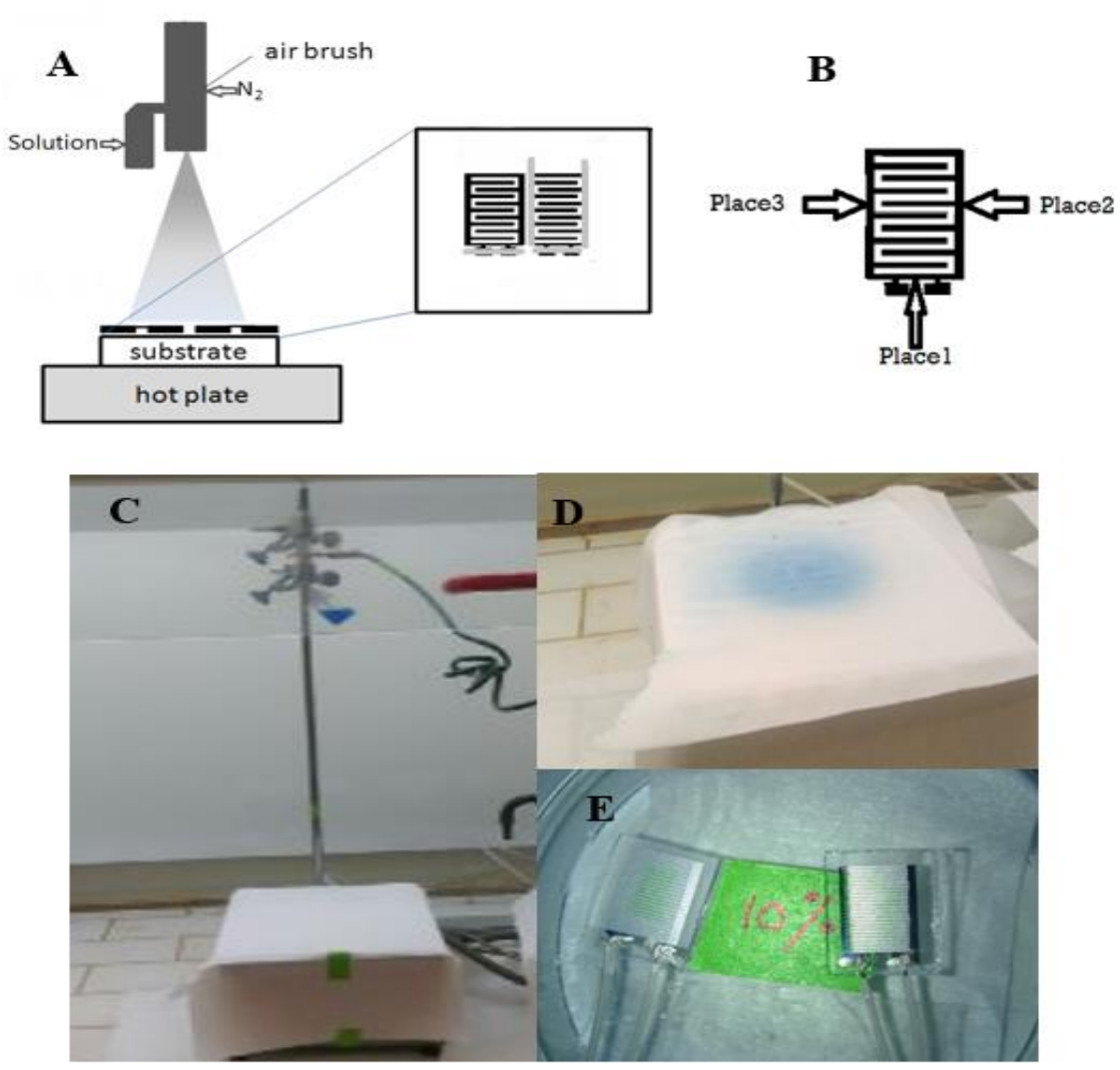

Fig.8. A**:** Schematic view of the Setup of aerosol spraying. B: Sample with marked position for measurement. C: Photo of the setup. D: Spraying colored solution to find out the most uniform place for spraying. E: A pair of sample with defined percentage right one is completely covered with nanoparticle left one has free edges

(**Fig. 8**E). To spot the most uniform position on top of the heater, colored liquid is sprayed and border of uniform place is defined (**Fig.8**D). Then the brush and flask needs to be completely cleaned with acetone and each pair of samples are located inside the border on top of the heater. Having mixed the solution in sonication for two minutes, based on the concentration of the nanoparticles of each solution, it was applied on each pair of the electrodes according to the aforementioned procedure.

2.2.6 PREPARATION OF SAMPLES FOR SEM IMAGING

Four samples with three nanoparticles concentrations of 40%, 60% and 50% with normal and heat treated were prepared. Generally, the preparation procedure is the same as the ones were mentioned for normal samples, just here substrate changed to be silicon, all the other details are similar. Also, after preparing the samples, they needed to be coated with a very thin layer of gold in order to prevent gathering of charges on the surface of dielectric film, which then will interfere with quality of the taken image.

2.3 RESULTS

2.3.1 THICKNESS OF THE DEPOSITED FILM

Thickness of deposited film was measured by profilometer in two or three places for each concentration in two different forms of fully covered with nanocomposite, F-Covered, and partially covered, P-covered, two edges of the electrode remained uncovered.

As it can be seen from the **Fig.9** the thickness varied from 7 µm to 30 µm for different concentrations. **Fig. 9** indicate the trend of thickness according to the percentage of ratio of the weight of nanoparticles to the weight of PMMA (concentration) for two repeated sets of the experiments. In **Fig.9**A the concentration of Nano particles starts 1 to 100%, and in **Fig.9**.B it starts from 10% up to 150%.

An upward trend for thickness of the deposited film is observed when percentage of the nanocomposite increases. Also, in most of the samples with same concentration percentage of nanoparticles, fully covered samples are thicker than partially covered. However, there are few points that does not follow this rule, which most probably occurs due to different errors during the experiment, including movement of brush or substrate while spraying, changing the pressure of nitrogen or not defining the correct place for having a uniform film.

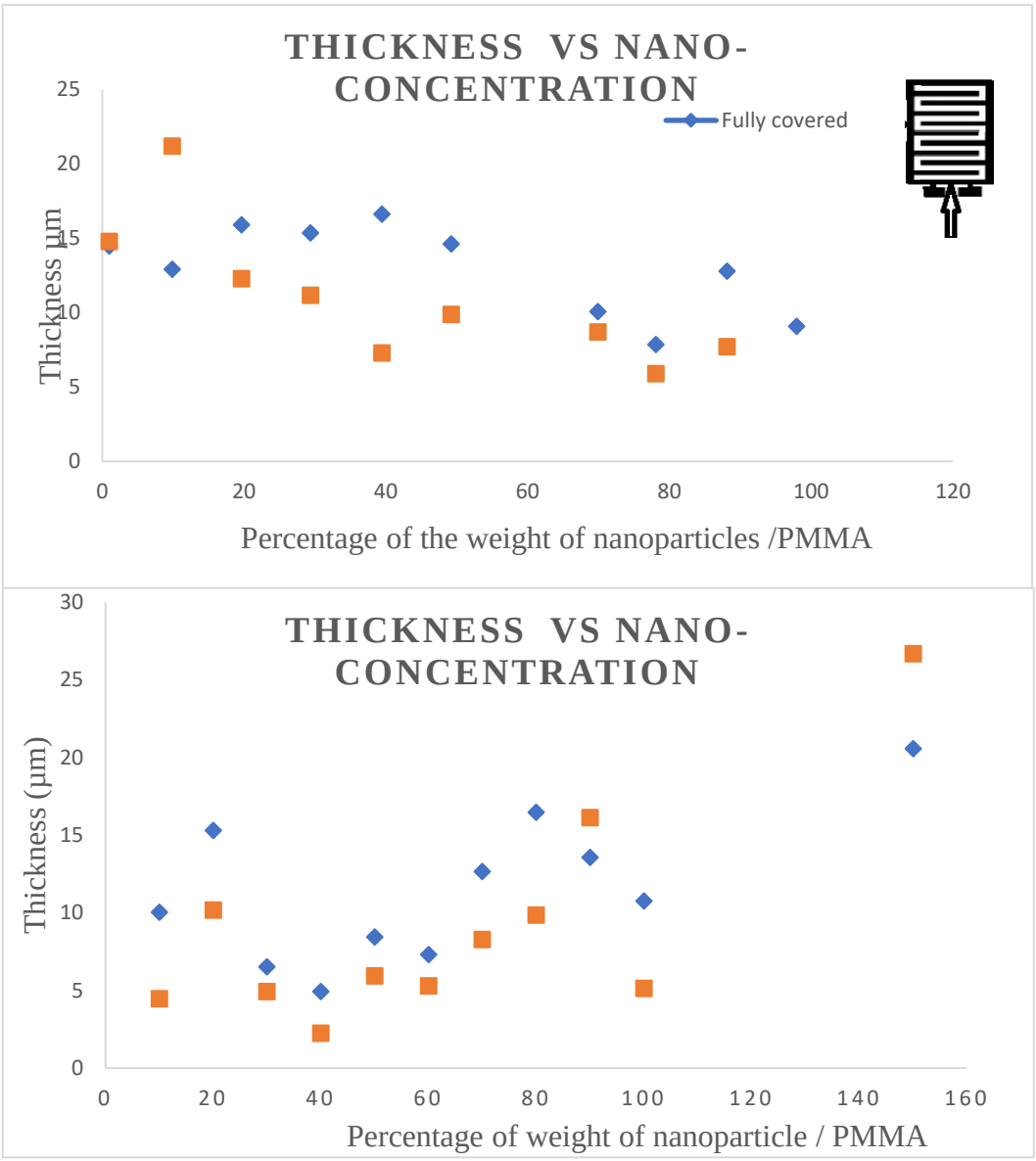

Fig.9. The thickness of deposited film in the indicated places versus their concentration of nanoparticles for fully covered and partially covered samples measured for two different sets.

Considering the obtained result and comparing it with the result from the earlier study related to this project, it is concluded that even though the used method for deposition of nanocomposite takes more time, but still it leads to a more uniform film than the method which was used previously. Previously the solution was sprayed on top of 10*10 cm^2 substrate including all printed electrodes which resulted in an ununiformed film considering its thickness. This ununiformed film caused a variance in electrical potential, which is very important parameter in the study.

2.3.2 VOLTAGE

To measure produced voltage out of exposing samples to humidity of the air, Keysight multi-meter Model 2000 was utilized. This Model has broad measurement ranges for DC voltage from 0.1μV to 1000V, DC current from 10nA to 3A, and two and four-wire resistance from 100μΩ to 120MΩ.

During the measurement in order to keep humidity under control samples was kept inside a small insulated chamber which got humidified with a small wet napkin. Having almost stabilized humidity, open circuit voltage, **Fig.10**, and voltage under 1 MΩ resistance, **Fig.11**, were measured and results were recorded.

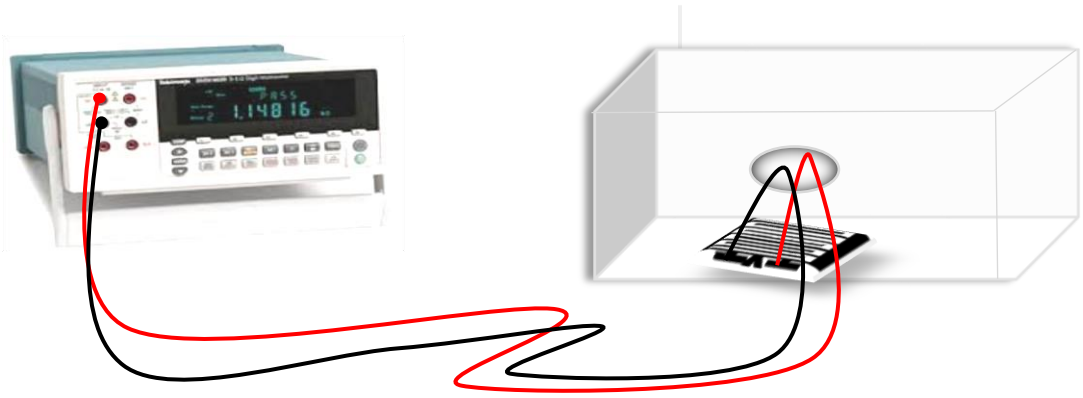

Fig. 10. Schematic view of the circuit for measuring open circuit voltage

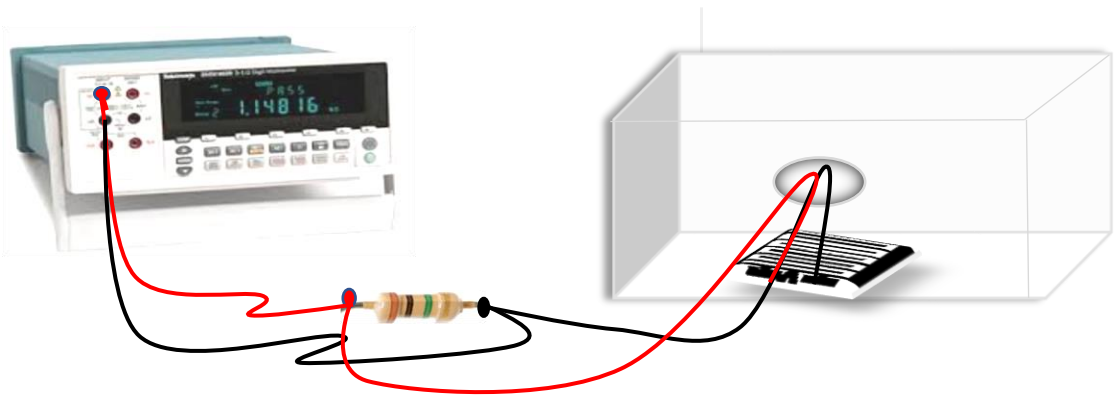

Fig. 11. Schematic view of the circuit for measuring voltage under 1 MΩ resistance

Fig.12 indicates measured voltage in case of open circuit for fully covered electrodes. It can be seen that in concentration of 10%, maximum amount of difference in electrical potential is achieved and other cases almost follow same behavior, they all shows voltage less than 100 mv at the beginning of the measurement which then slightly decreased during the time. In case of 40% at the beginning of the measurement voltage is -300 mv but after passing short amount of time the polarity of the voltage changed and after two hours of measurement it shows voltage around 100 mv. However, with comparing the amount of humidity (**Table.1**) in case of 10% nanoparticle concentration with other concertation it can be concluded that the difference in the measured voltage between different concentrations is related to humidity level.

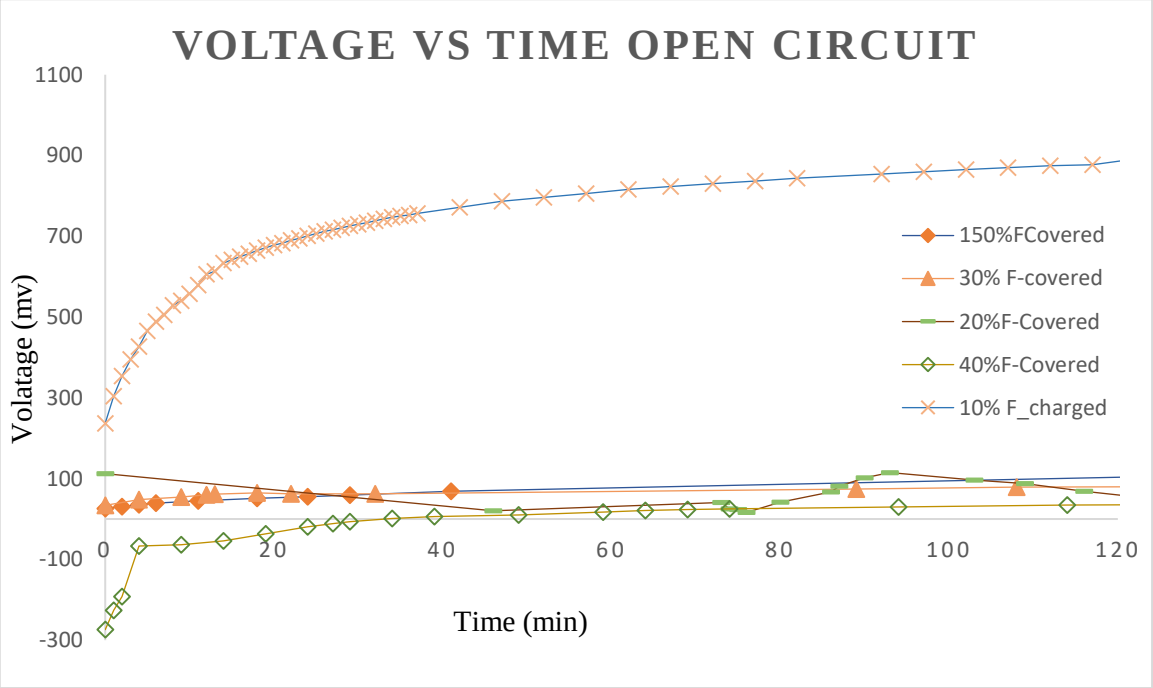

Fig.12. Measurement of the voltage in open circuit for different concentrations in case of fully covered electrodes.

Table 1. Relative humidity and temper in case of open circuit for fully Covered electrodes

Concentration	Av-Hum	Av-Tem
150%F-Covered	71.78	20.4
90%F-Covered	76.6	21.1
30%F-Covered	80.2	22.37
10%F-Covered	55.6	19.4

20%F-Covered	71.1	25.1
40%F-Covered	80.9	21.4

Same measurement was conducted for partiality covered electrodes, from the **Fig.13** it is seen that measured voltage is less in comparison to fully covered electrodes. Relative humidity level for this parts of measurement is more than 70%. Samples with concentration of 60% and 50% follow almost similar trend, they both at first shows almost zero voltage but after passing 40 minutes, level of the measured voltage in both of them increased to more than 100 mv. Despite the fact that 90% concentration acts differently from the others but after 40 minute, all of the concentrations follow similar rule and reach to about 100 mv.

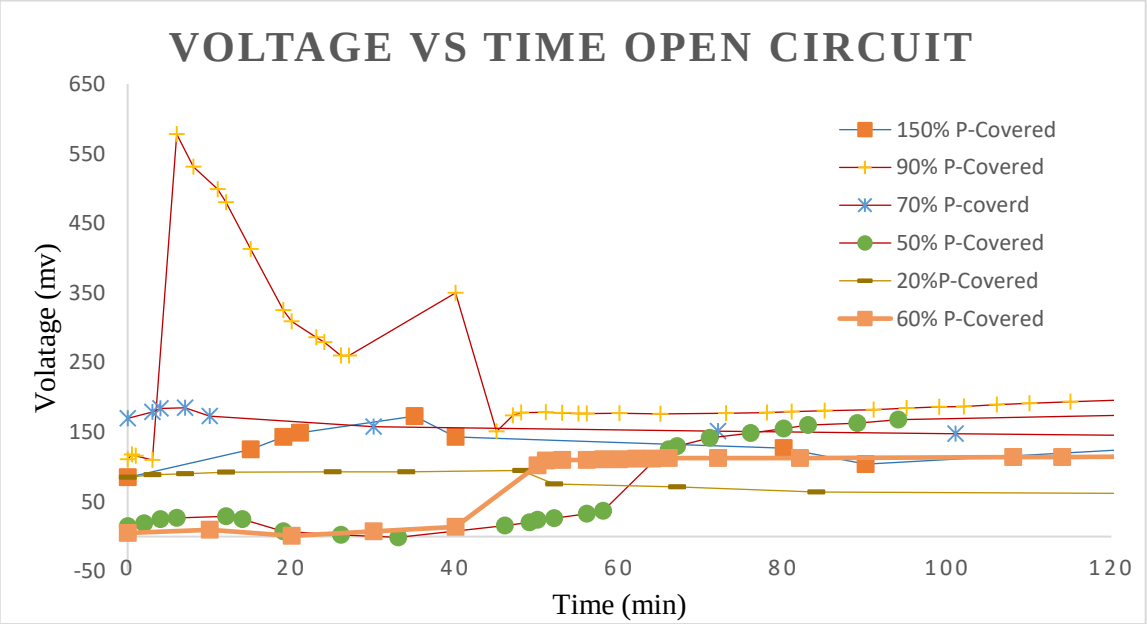

Fig.13. Measurement of the voltage in open circuit for different concentrations in case of partially covered electrodes

Table 2. Relative humidity and temperature in case of open circuit for fully covered electrodes

Concentration	**Av-Hum**	**Av-Tem**
150%P-Covered	78.48	21.6
90%P-Covered	75.6	22.6

70%P-Covered	71.78	21.7
50%P-Covered	78.8	24.2
20%P-Covered	81.6	20.59
60%P_covered	77.8	20.9

Process of exposing samples to the humidity of the air is similar to charging of capacitor, so with adding resistance to the circuit it is expected to see similar behavior as discharging. **Fig.14** shows the changes in measured voltage in circuit with 1MΩ load in case of fully covered electrodes.

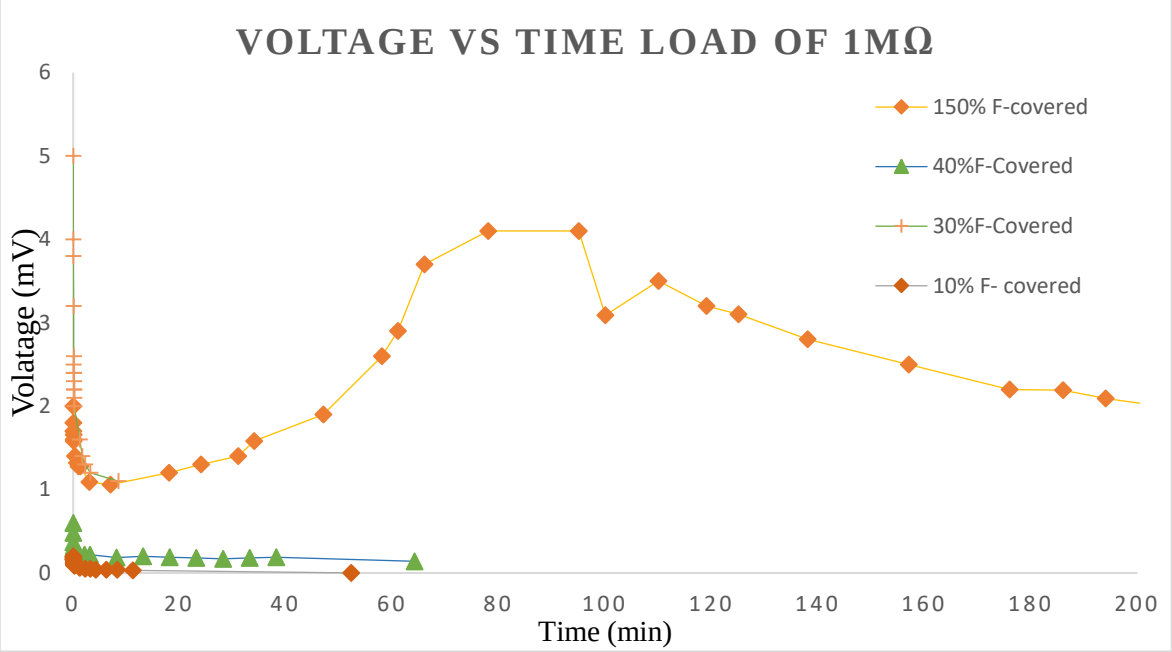

Fig.14. Measurement of the voltage in circuit with load of 1MΩ for different concentrations in case of fully covered electrodes.

Form **Fig.14**, it can be seen that highest value for voltage resulted 150% and 30% and for other concentration voltage starts from several mv and then very fast dropped to zero. Relative humidity level during the measurement as an average, change from 74% for 10% concentration to 81% for 40%.

Table 3. Relative humidity and temperature for circuit with load of 1MΩ for fully covered electrodes.

Concentration	Av-Hum	Av-Tem
150%F-Covered	76.09	21
30%F-Covered	80.9	20.9
10%F-Covered	74.67	21.442
40%F-Covered	81.2	21.455

Results for case of partialy covered electrods shows (**Fig.15**) higher voltage than in case of fully covered one. At the beginning of the measurment, 60% has highest voltage in comaprison to other concentration but as time passed 50% indicates higher result.

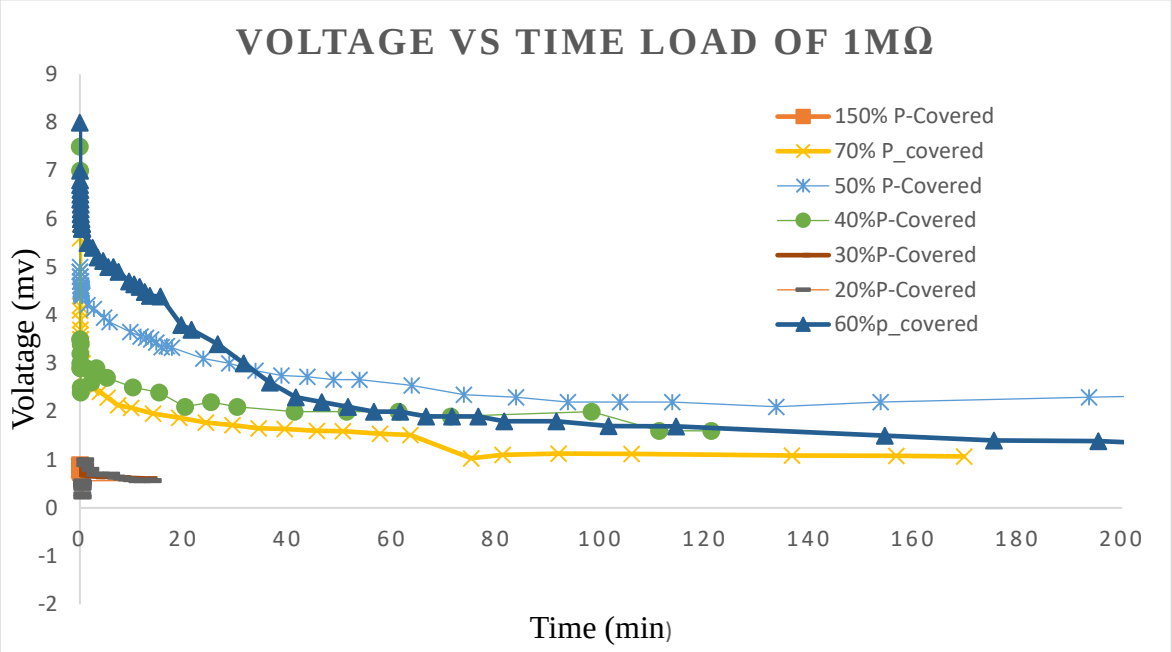

Fig. 15. Measurement of the voltage in circuit with load of 1MΩ for different concentrations in case of partially covered electrodes.

Table 4. Relative humidity and temperature for circuit with load of 1MΩ for partially covered electrodes

Concentration	Av-Hum	Av-Tem
150%P-Covered	78.482	21.685
70%P-Covered	79.525	21.75
50%P-Covered	80.393	21.09
30%P-Covered	81.54	21.6
20%P-Covered	81.62	20.593
40%P-Covered	79.88	22.7
60%P_covered	77.85	20.90

Average humidity level and temperature were mentioned in **Table 1-4** for open and under load circuit, also in **Fig.16** & **17** trend of their changes are shown. It is seen that average humidity and temperature are almost at the same level and it varies form 71% - 76% to 77% - 81%; and average temperature varies from 19℃ and 20℃ to 25℃ and 21℃ in case of open circuit and for circuit with load of 1MΩ, respectively.

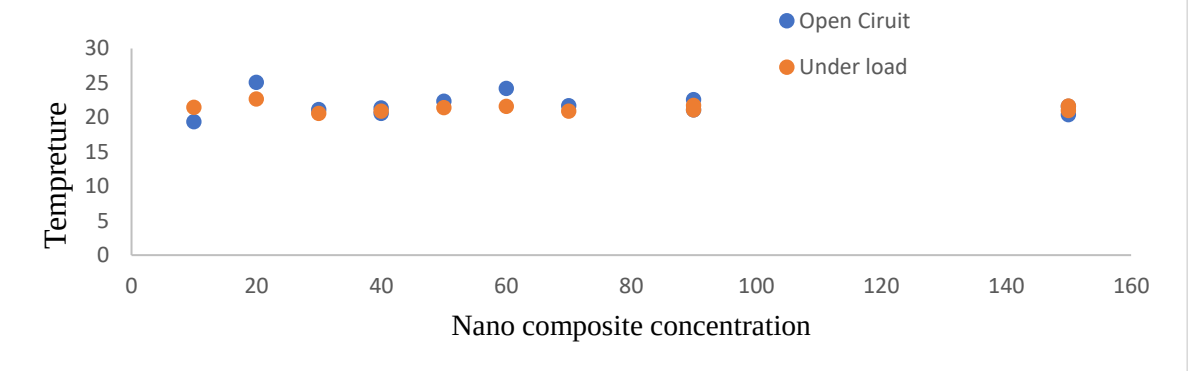

Fig.16. Trend of change in temperature while measuring voltage under load and open circuit

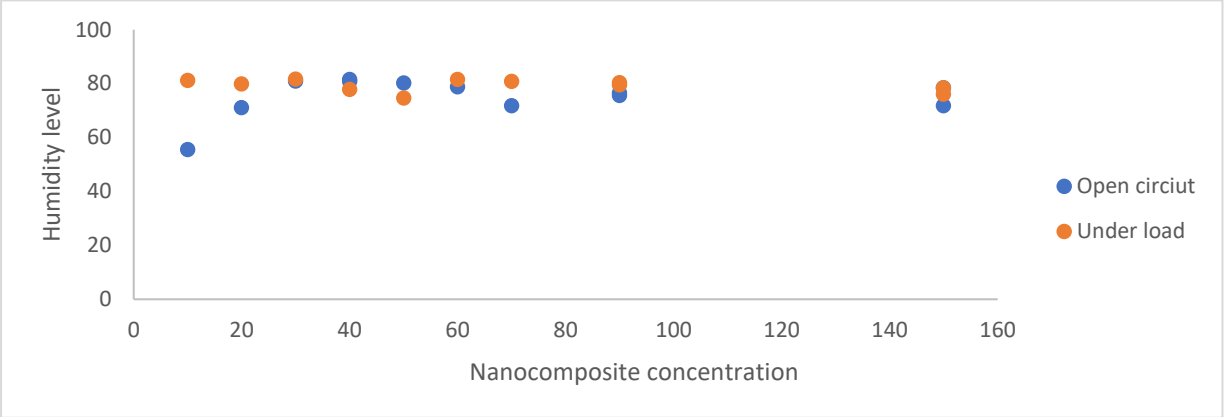

Fig.17. Trend of change in humidity level while measuring voltage under load and open circuit

During the voltage measurement some of the samples get destroyed. For instance due to high level of humidity the deposited film got detached from the surface. This especially happened after open circuit and as a result some of samples was not measured for case of under load.

2.3.3 ANALYSIS OF THE DATA AND CONSTRUCTING A MODEL

To analysis data collecting from different experiments conducted during this study, multiple regression is applied and humidity, temperature, and duration of measurement considered to be potential independent variables and produced voltage as dependent variable.

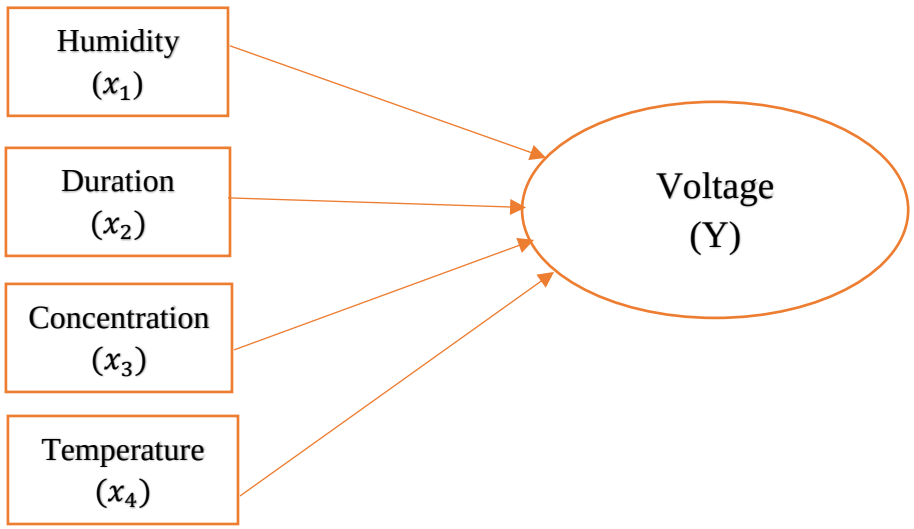

In order to confirm the dependent and independent variables in the first stage correlation between all independent variable should be monitored. In Table.6 regression coefficient and P-value for different potential dependent variables are mentioned, P-values determines statistical significance in a hypothesis test, it measures how compatible the data is with the null hypothesis when P values is high null hypothesis is likely to be true and in case of low P values null hypotheses is rejected [21].

Table 5. Correlation between all dependent variables

Null hypotheses	Coefficient	P-value	Reject /accept
Humidity is dependent on duration	0.00059	0.064102371	Rejected ×
Humidity is dependent on Temperature	-0.0808	0.0183	Rejected ×
Humidity is dependent on concentration	0.08325	0.000	Rejected ×
Temperature is dependent on time	-0.00032	0.09262	Rejected ×
Temperature is dependent on time	-0.00032	0.09262	Rejected ×
Temperature is dependent on Concentration	0.000	0.883808	Rejected ×
Time is dependent on concentration	0.000	0.883808	Rejected ×

Considering the very small coefficient in most cases despite the fact that in some of the cases P-value is also enough small to shows that there is dependency between the above-mentioned variables, all of them can be considered independent (**Table.5**).

If we apply the regression model to all our data, we cannot find a unique model to fit our extracted data. Considering the fact that concentration is one of the most significant factors in these experiments, in the following it is shown, and there are two opposite trends for the amount of produced voltage based on the concentration of nanoparticle, from 10% to 50% there is an upward trend while from 50% to 90% this change to be downwards trend.

Accordingly, we fit a regression model for 10% to 50% and separately from 50% to 150% of concentration of nanoparticle in the applied film on top of aluminum electrodes.

Considering the analyzed data for 70% and 60% of concentration nanoparticles with correct predication of 68% below bullet points can be extracted:

- Very strong negative correlation between concentration and output voltage (-68.47)
- Strong positive correlation between humidity and output voltage (2.39)
- Weak negative correlation between temperature and output voltage (-0.26, range 19.2-23.3)
- Very weak negative correlation between time and output voltage (-0.009)

In addition, for 20%-50% of concentration nanoparticles with correct prediction of about 78% below bullet points can be extracted:

- Very strong positive correlation between concentration and output voltage (14.35)
- Positive correlation between humidity and output voltage (0.68)
- Very weak positive correlation between temperature and output voltage (0.005). This value is more likely to be random as a result it will neglected that in the final formula
- Very weak negative correlation between time and output voltage (-0.0011)

2.3.4 STUDY OF BEHAVIOR OF SAMPLES BASED ON HUMIDITY LEVEL

According to the previous part of the study and related analysis, second most important factor in the output voltage is humidity, in this part of study concentration is fixed and humidity level changes to see the result for output voltage. A sample with concentration of 50% according to the same procedure mentioning in the sample preparation sections got ready and voltage for open circuit and under load of 1MΏ , considering different humidity level, 53-55% , 56-60%, 66-70%, 73-76% and 76-89% separately each for more than 2 hours was measured. As it can be seen from the **Fig.18 19** maximum amount of voltage in either cases of open circuit voltage and circuit with resistances occurs at relative humidity around

76%. In case of open circuit it looks that when humidity level is lower, amount of voltage is higher which most probably is due to statistic charges which can be formed much better when the air is dry or the humidity is low.

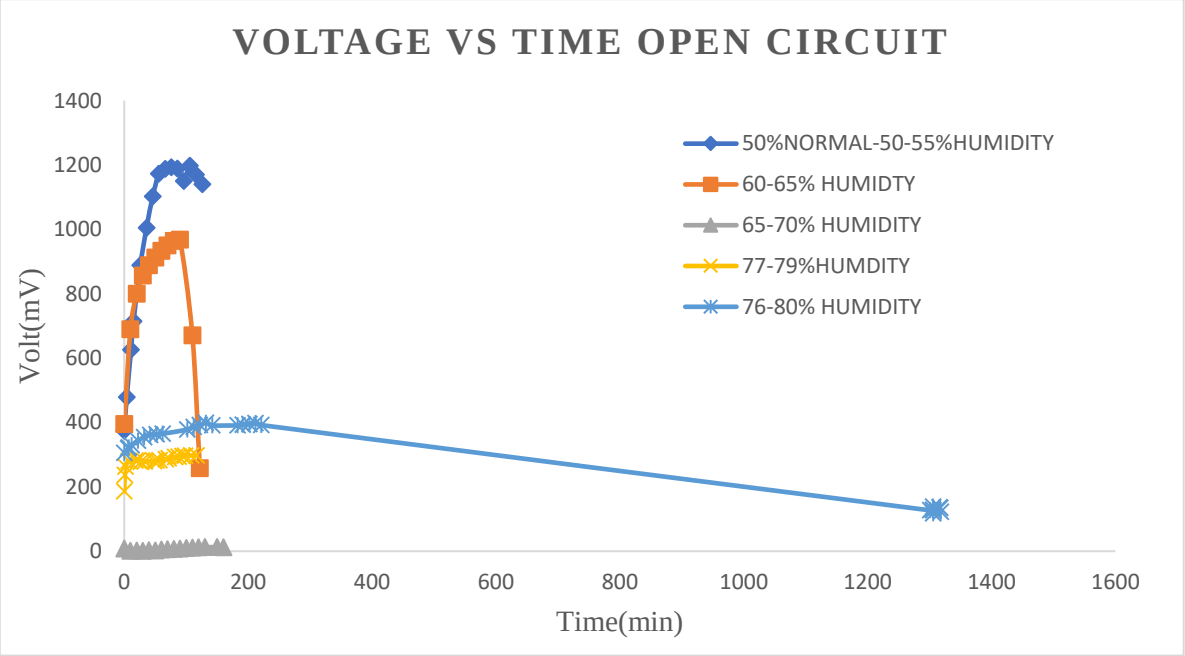

Fig.18. Values of voltage in open circuit for different relative humidity level

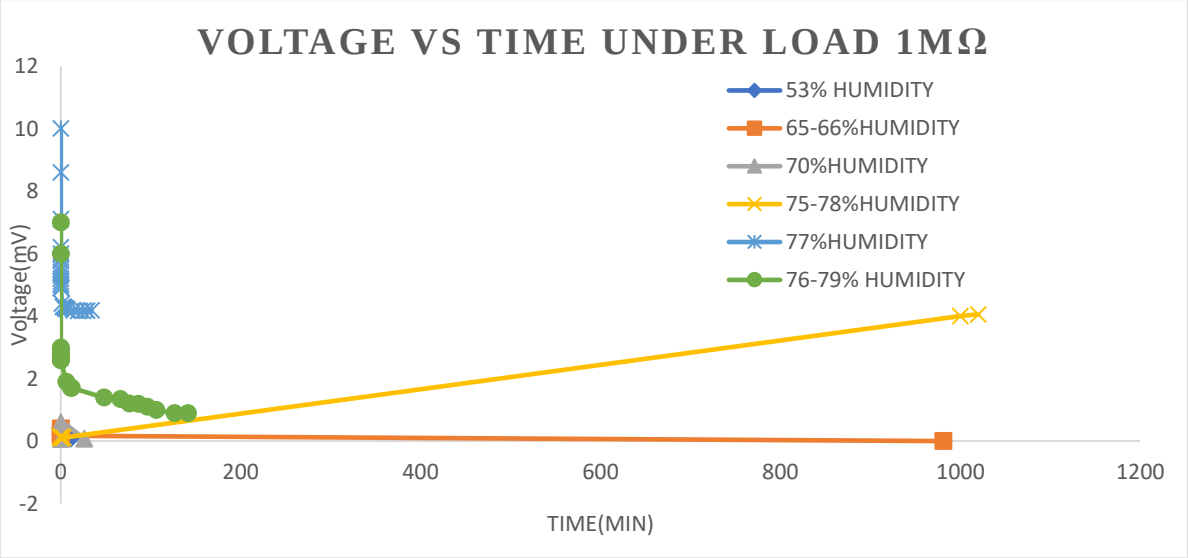

Fig. 19. Values of voltage in circuit with load of 1 MΩ for different relative humidity level

2.3.5 HEAT TREATED NANOPARTICLES

Considering the result and analysis, it is understood that the highest value for voltage is obtained for 50% concentration nanocomposite. However, this result was concluded mostly from the measured voltage from circuit with resistance of 1MΩ, as in case of open circuit there was more possibility of having errors due to measuring instrument and wiring and also statistic charges which could have a deep influence on final result. Accordingly, it was planned to make a sample with 50% concentration of $Z_2O_2 - 3Y_2O_3$ and treat it with heat to see the difference and compare the result. Thermal treatment caused an increase in the size of crystal of zirconia. Boosting the temperature by 300–500 °C can end to a particle size of three or even four times more than the original [22]. For this purpose some amount of $Z_2O_2 - 3Y_2O_3$ (TZP) nanoparticles left in furnace with 700 °C for two hours. The heating rate was 5 °C/min. Then these preheated nanoparticles applied on to the aluminum electrode with the same method as previous samples.

The measurements indicates an increase in voltage for heat treated nanocomposite in either under load and open circuit voltage comparing with 40% and 60% concentration, seen on **Fig. 20 & 21**.

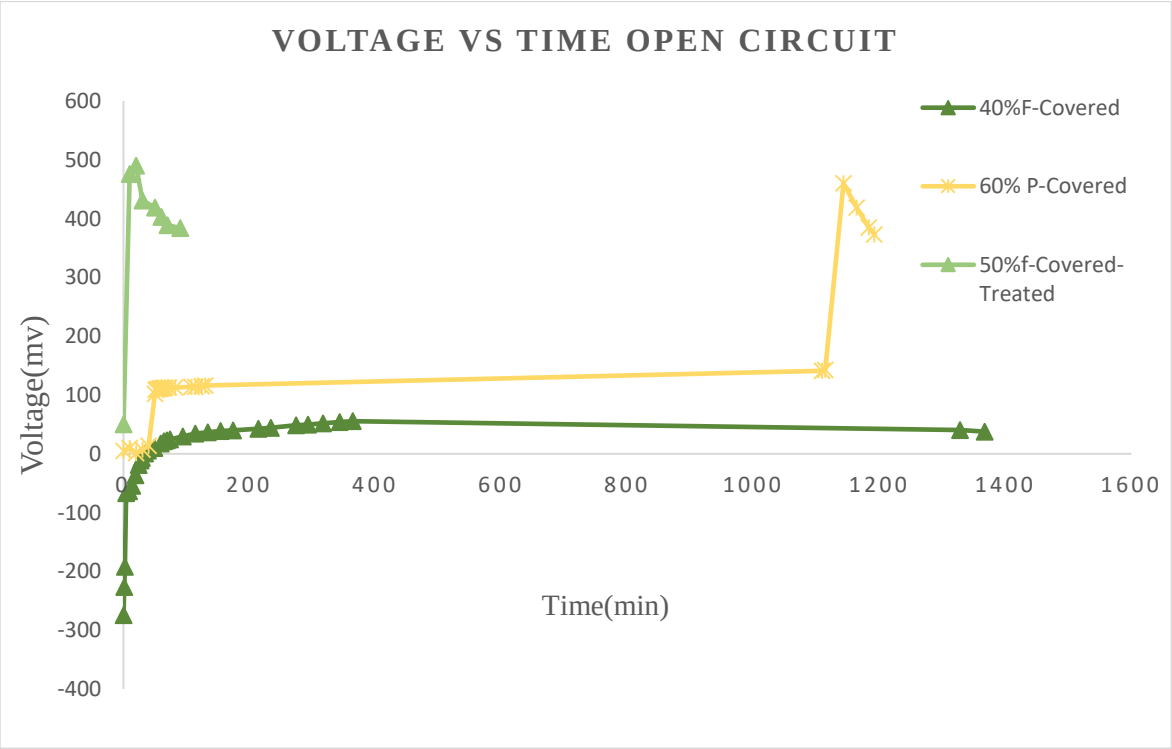

Fig.20. Measurement of the voltage in open circuit for different concentration

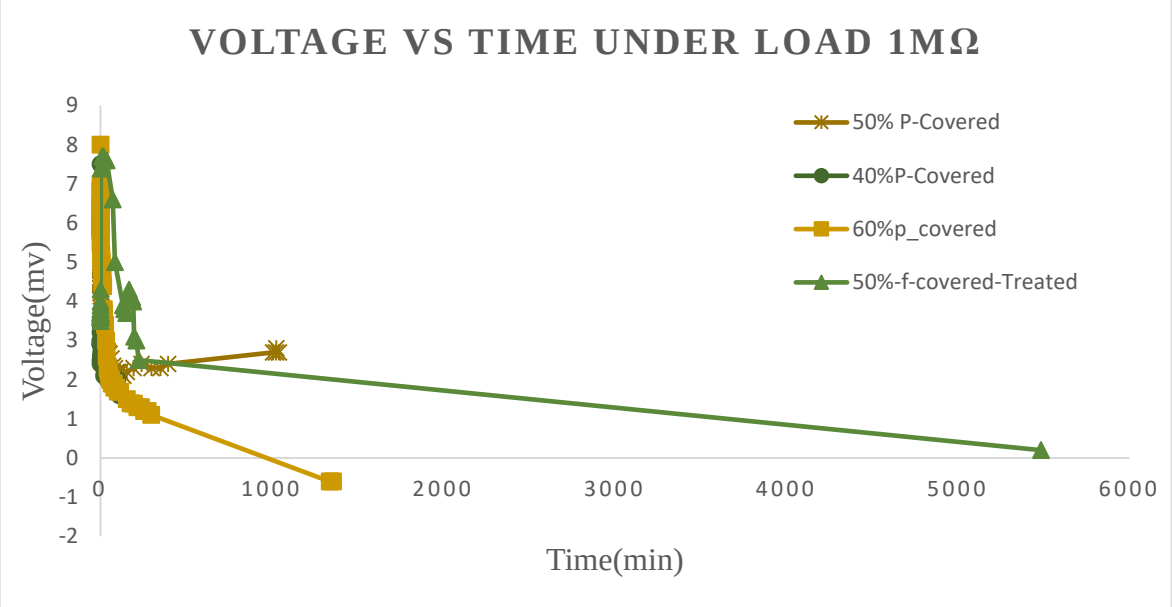

Fig.21. Measurement of the voltage in a circuit with load of 1 MΩ

2.3.6 SEM IMAGING

SEM images from samples with 40%, 50% and 60% concentration of nanoparticle were captured. SEM imaging in **Fig.22** indicates agglomeration in the applied film on top of electrodes. Additionally, sample with 50% concentration of nanocomposite that was assumed to have the highest electrical output among the studied samples, appeared to show the most uniform distribution of nanoparticles of the solution within the value of the coating.

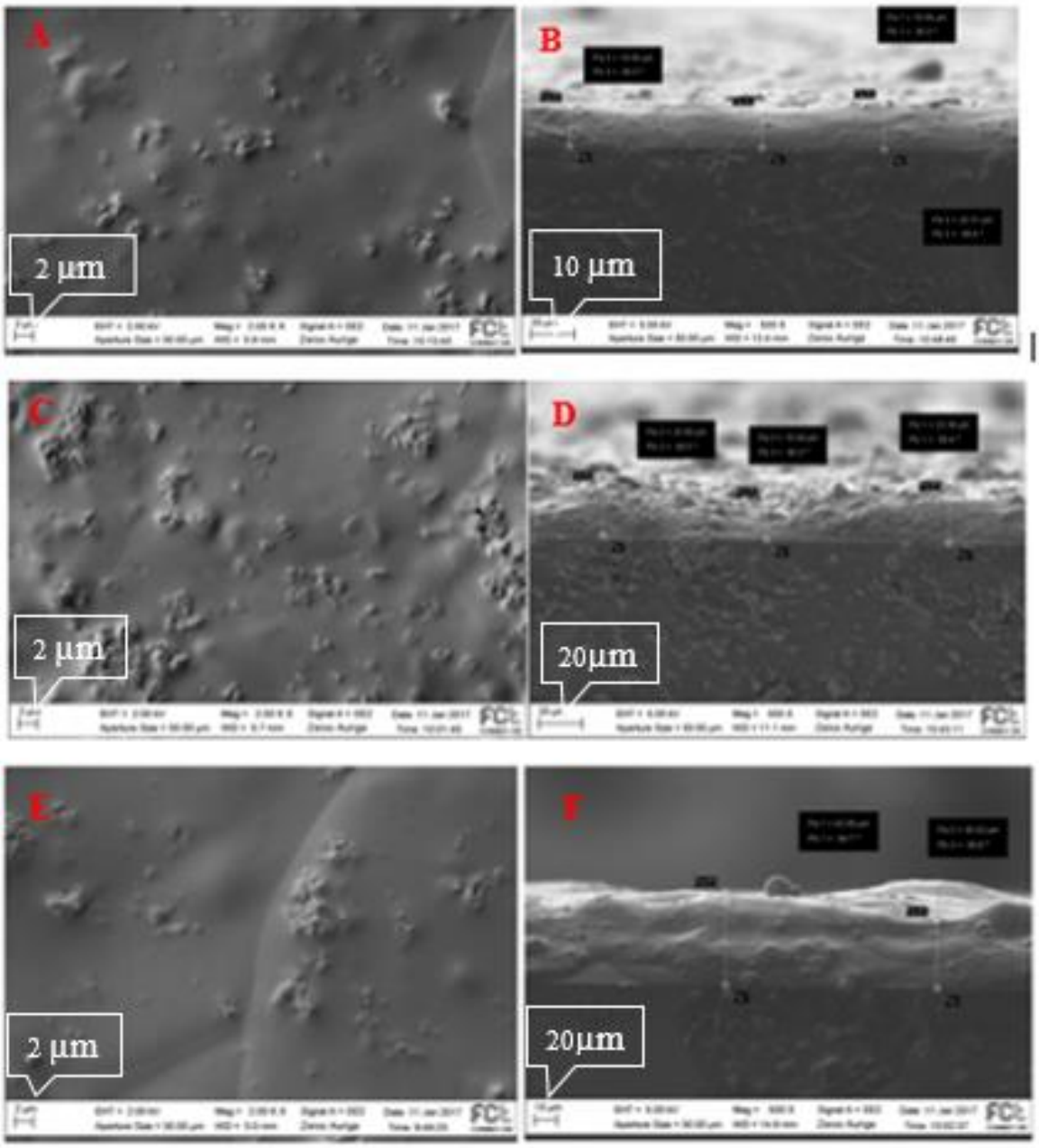

Fig. 22. A: SEM image for 40% concentration of Nano composite, from surface. B: SEM image for 40% concentration Nano composite for cross section. C: SEM image for 50% concentration from surface. D: SEM image for 50% concentration of Nano composite from cross section. E: SEM image for 60% concentration of Nano composite from surface. F: SEM image for 60% concentration from cross section.

2.3.7 SPECTROSCOPY

Backscattered electrons can produce compositional contrast in SEM images due to different atomic number elements and their distribution. Also, Energy Dispersive Spectroscopy (EDS) can determine particular elements and their relative proportions. For 50% nanocomposite concentration backscattered electron image and EDS spectroscopy was conducted and the result is displayed in **Fig. 23**.

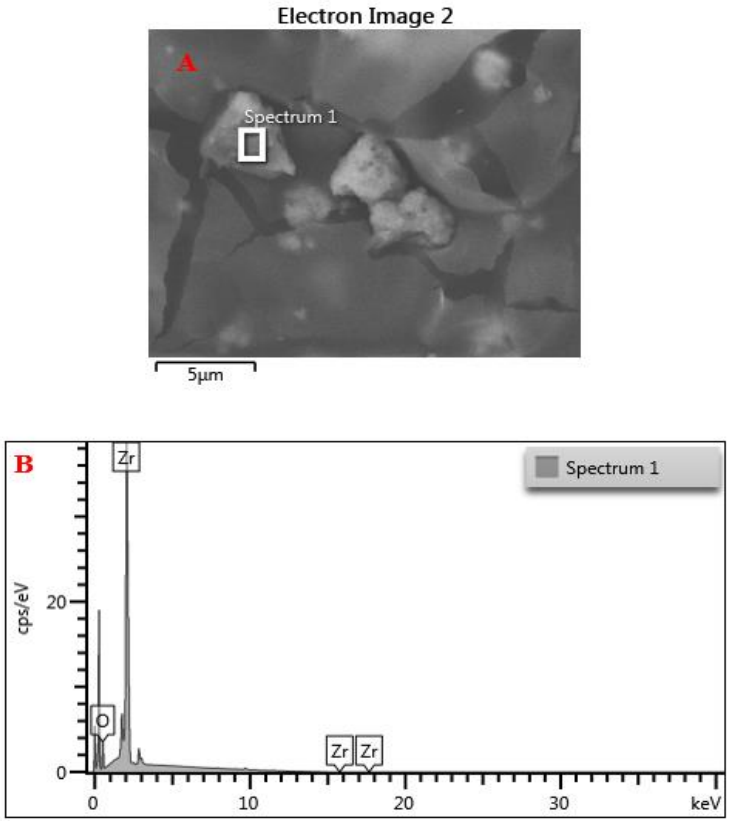

Fig.23. For 50% nanocomposite concentration A: Backscattered electron image showing the contrast, B: Energy Dispersive Spectroscopy

Elemental mapping of the surface and cross section of the sample with 50% concentration of nanoparticle are shown at Fig.24A& B. From the figures it can be conclude that in the agglomerated part of the ZrO_2 nanoparticles there is a stacking of zirconium and in other places there is much less amount of zirconia, is distributed along the film. Also cross-section image from 50% in Fig.24B indicates that inside the film zirconium is distributed relatively uniformly.

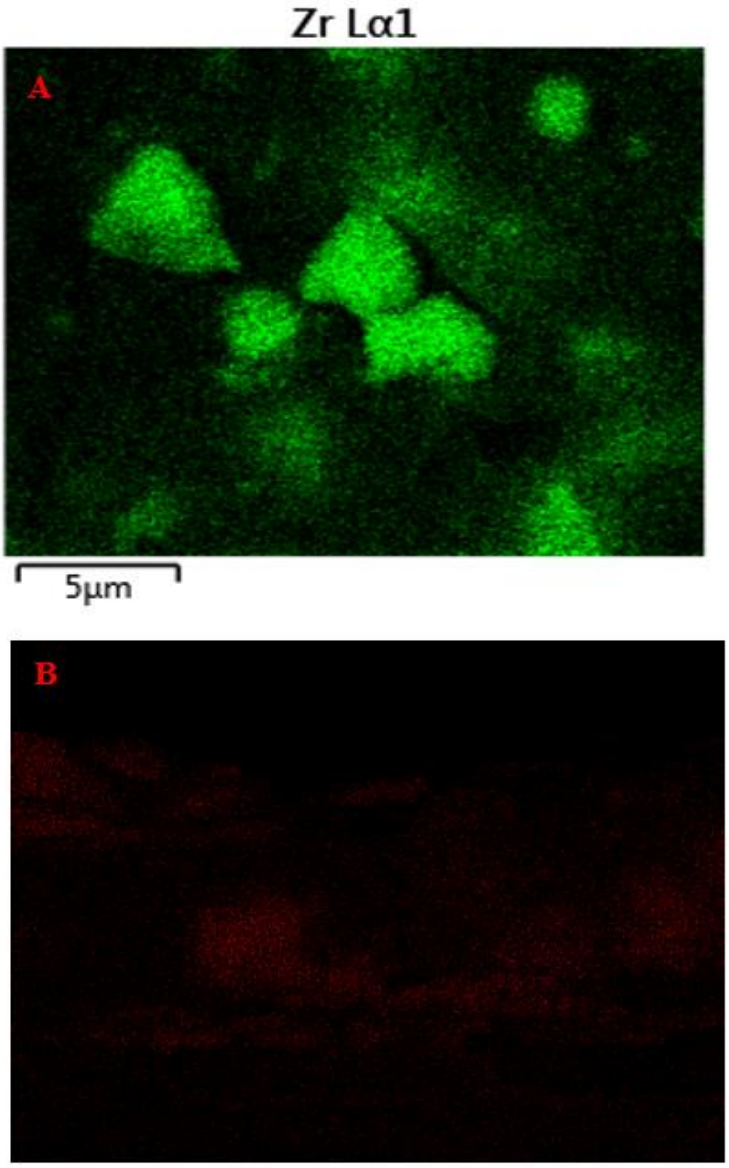

Fig.24. A: Elemental mapping from surface of the 50% concentration sample, green dots indicate zirconium. B: Elemental mapping from cross-section of the sample with concentration of ZrO_2 50%, red dots indicate zirconium atoms.

3 DISCUSSION AND CONCLUSIONS

This thesis developed an innovative method based on interaction of ZrO_2 Nano powder to produce energy out of humidity of the air. During this study bellow conclusions were reached

1. Measurement of thickness of deposited nanocomposite on top of aluminum electrodes show almost a uniform film covering each sample. Also it was indicated that thickness of deposited film shows an increase with increasing amount of nanoparticle, ZrO2+3mol%Y2O3, in comparison to PMMA.
2. It was observed that output voltage in two different circuit without and with load of 1MΩ, has a strong correlation with the amount of zirconia nanoparticle. Highest value for voltage can be obtained for 50% concentration, weight of zirconia Nano power is half PMMA.
3. Humidity as the second most effective factor in producing energy shows strong correlation with voltage. Considering the result of the study on humidity level for three concentration of nanoparticle, 40%, 50% and 60%, it was shown that around 76% relative humidity the voltage shows higher value. This character, that changes in the level of relative humidity can change the amount of produced voltage can be utilized for humidity sensor.
4. Thermal treated $Z_2O_2 - 3Y_2O_3$ (TZP) nanoparticle, powder in furnace with 700 °C for two hours, shows higher value for output voltage and electrical current in comparison to the one not be treated with heat.
5. SEM imaging form samples with 40%, 50%m and 60% concentration of TZP nanoparticle shows that in case of 50% there is a more uniform distribution of nanoparticle and less agglomeration is observed. This observation could be considered as the reason for having higher voltage and current in case of 50% nanoparticle concentration.
6. EDS spectroscopy and elemental mapping of sample with 50% concentration of nanoparticle shows more number of zirconia nanoparticles in agglomeration part in comparison to other part of the film. Also elemental mapping from cross section of the sample indicates more uniform distribution of zirconia nanoparticle inside the sample.

The importance of this study lay down in developing a method to directly convert adsorbed gas-phase water to electric energy. However in order to move further in this study the exact mechanism of the produced energy out of the interaction of TZP nanoparticle with humidity of the air need to be fully understood. For this purpose measurement of surface potential and charge distribution on surface of the sample with AFM, Atomic Force Microscopy, and KPFM, Kelvin Probe Force Microscopy, can be very informative.

Despite several efforts to have stabilize humidified environment to make measurement with AFM, it was not achieved during this study due to shortage of time and due to technical problem. Also in order to confirm the results from this study some parts of that needs to be repeated to check the repeatability and reproducibility of the achieved result. In addition, studying agglomeration of nanoparticles and finding out a proper to prevent it might has a great effect in improving the efficiency of the produced energy.

4 SUMMARY

This thesis was a part of EU project named HUNTER, aiming to convert humidity of the air to electricity. Working as a member of an international research team provided me with great opportunity to improve my communication skills while I was learning scientific knowledge. Practical parts of this study supply me to with valuable experience in

- Working with chemical material and equipment to fabricate and pretreat different combination of nanocomposite from TZP nanoparticles.
- Working in clean room to deposit aluminum on glass substrate by vapor deposition method
- Working in clean room to conduct lithography on the aluminum substrate to fabricate electrodes which then was used to be substrate for the nanocomposite solution deposition.
- Getting familiarized with SEM imaging equipment
- Getting familiarized to work with AFM equipment

5 REFERENCES

1. Soares, L.C. et al., 2008. A new mechanism for the electrostatic charge build-up and dissipation in dielectrics. *Journal of the Brazilian Chemical Society*, 19(2)
2. Ducati, T.R.D., Simões Luís H. & Galembeck, F., 2010. Charge Partitioning at Gas−Solid Interfaces: Humidity Causes Electricity Buildup on Metals. *Langmuir*, 26(17), pp.13763–13766.
3. Boreyko, J.B. & Chen, C.-H., 2009. Self-Propelled Dropwise Condensate on Superhydrophobic Surfaces. *Physical Review Letters*, 103(18).
4. R. Enright. N. Miljkovic, J. Sprittles, R. Mitchell, K. Nolan, and E. N. Wang., 2014. How coalescing droplets jump. ACS Nano, 8 (10).
5. Miljkovic, N. et al., 2014. Jumping-droplet electrostatic energy harvesting. Applied Physics Letters, 105(1), p.013111.
6. Doroshkevich, A.S. et al., 2017. Nonequilibrium chemo-electronic conversion of water on the nanosized YSZ: experiment and Molecular Dynamics modelling problem formulation. *Journal of Physics: Conference Series*, 848, p.012021.
7. Massalski, T.B. et al., 1992. *Binary alloy phase diagrams*, S.l.: ASM International, 2940-2941.
8. Lvov, S.N., 2007. Electrochemical Techniques for Studying High-temperature Subcritical and Supercritical Aqueous Solutions. *Encyclopedia of Electrochemistry*.
9. Affatato, S.; Ruggiero, A.; Merola, M. Advanced biomaterials in hip joint arthroplasty. A review on polymer and ceramics composites as alternative bearings. *Composites Part B: Engineering* **2015**, *83*, 276–283.
10. Kong, L. B.; Huang, Y.; Que, W.; Zhang, T.; Li, S.; Zhang, J.; Dong, Z.; Tang, D. Sintering and Densification of Transparent Ceramics. *Transparent Ceramics Topics in Mining, Metallurgy and Materials Engineering* **2015**, 467–517.
11. Garvie, R. C. The Occurrence of Metastable Tetragonal Zirconia as a Crystallite Size Effect. *The Journal of Physical Chemistry* **1965**, *69*, 1238–1243.
12. Alekseenko, V.I. & Volkova, G.K., 2000. An adsorption mechanism underlying phase transformation in stabilized zirconia. *Technical Physics*, 45(9), pp.1154–1158.

13. Kogler, M. et al., 2014. Hydrogen Surface Reactions and Adsorption Studied on Y2O3, YSZ, and ZrO2. *The Journal of Physical Chemistry C*, 118(16), pp.8435–8444.
14. Anon, 2015. The Difference Between Positive and Negative Photoresist |. *Shin-Etsu MicroSi*. Available at: https://www.microsi.com/the-difference-between-positive-and-negative-photoresist/ [Accessed August 7, 2017].
15. Anon, Photoresists. *www.microchemicals.com/de*. Available at: http://www.microchemicals.com/products/photoresists.html [Accessed August 7, 2017].
16. Anon, 1970. Top Down Approach. *Nanotechnology*. Available at: http://www.nanotechandsensors.com/2015/07/top-down-approach.html [Accessed August 7, 2017].
17. Reed, S.J.B., Introduction. *Electron Microprobe Analysis and Scanning Electron Microscopy in Geology*, pp.1–6.
18. Anon, Research and Economic Development. *UI Central Microscopy Research Facility ready to help investigators win grants | Research and Economic Development | The University of Iowa*. Available at: https://research.uiowa.edu/impact/news/ui-central-microscopy-research-facility-ready-help-investigators-win-grants [Accessed August 7, 2017
19. Agron, P., Fuller, E. & Holmes, H., 1975. IR studies of water sorption on ZrO2 polymorphs. I. *Journal of Colloid and Interface Science*, 52(3), pp.553–561.
20. Liu, R. & Wang, C.-A., 2013. Effects of mono-dispersed PMMA micro-balls as pore-forming agent on the properties of porous YSZ ceramics. *Journal of the European Ceramic Society*, 33(10), pp.1859–1865.
21. Baker, M., 2016. Statisticians issue warning over misuse of P values. *Nature*, 531(7593), pp.151–151.
22. Mercera, P. et al., 1990. Zirconia as a support for catalysts. *Applied Catalysis*, 57(1), pp.127–148.